Optimizing Cell Permeation of an Antibiotic Resistance Inhibitor for Improved Efficacy

Alberto Venturelli,[†] Donatella Tondi,[†,‡] Laura Cancian,[†] Federica Morandi,[†,‡] Giuseppe Cannazza,[†] Bernardetta Segatore,[§] Fabio Prati,[‖] Gianfranco Amicosante,[§] Brian K. Shoichet,[‡] and M. Paola Costi*,[†]

Dipartimento di Scienze Farmaceutiche, Università degli Studi di Modena e Reggio Emilia, Via Campi 183, 41100, Modena, Italy, Department of Pharmaceutical Chemistry, University of California, San Francisco, 1700 4th Street, Byers Hall N508D, San Francisco, California 94158-2330, Dipartimento di Scienze e Tecnologie Biomediche, Biochimica Clinica e Biologia, Molecolare Clinica, Università degli Studi de L'Aquila, Via Vetoio 10, 67010, L'Aquila, Italy, and Dipartimento di Chimica, Università degli Studi di Modena e Reggio Emilia, Via Campi 183, 41100, Modena, Italy

Benzo[*b*]thiophene-2-ylboronic acid, **1**, is a 27 nM inhibitor of the class C β-lactamase AmpC and potentiates the activity of β-lactam antibiotics in bacteria that express this and related enzymes. As is often true, the potency of compound **1** against the enzymes is much attenuated in cell culture against Gram negative bacteria, where the minimum inhibitor concentration of compound **1** is in the mid-micromolar range. Here, we modulated the properties of this lead to enhance its ability to cross the membrane, using a combination of X-ray crystallography, structure-based design, and application of physical models of outer membrane crossing. This strategy led us to derivatives with substantially improved permeability. Also, the greater solubility of these compounds allowed us to measure their efficacy at higher concentrations than with the lead **1**, leading to higher maximum potentiation of the antibiotic effect of ceftazidime on resistant bacteria.

Introduction

β-Lactamases are the most pervasive resistance mechanism to β-lactam antibiotics, such as the penicillins and cephalosporins, acting to hydrolyze and consequently inactivate these drugs. Of particular clinical relevance are chromosomally encoded class C β-lactamases that are expressed by some *enterobacteria* and *pseudomonas.* For these enzymes, β-lactam-based inhibitors such as clavulanic acid or sulbactam are ineffective and "β-lactamase stable" β-lactams, such as ceftazidime, are recognized as substrates.[1−4] Indeed, some pathogens have evolved mechanisms that, in the presence of primary β-lactams or β-lactam-based inhibitor, up-regulate the expression of the very β-lactamases that they were designed to evade or inhibit.[5,6]

The broad activity of class C β-lactamases against and the regulatory response to classic β-lactams has motivated a search for novel inhibitors structurally unrelated to β-lactams. Such non-β-lactam inhibitors might be able to evade pre-evolved bacterial resistance mechanism: they would not be recognized by β-lactam signaling proteins, might not be affected by porin channel mutations, responsible for decreasing permeability, and, lacking the β-lactam core, they should not be hydrolyzed by mutant enzymes that arise in response to new β-lactams.[6−10] Using both structure-based[11−13] and transition-state analog approaches,[7] several such novel inhibitors have been developed. Among the more potent of these is benzo[*b*]thiophene-2-ylboronic acid (compound **1**, Figure 1),[11] which inhibits the canonical class C β-lactamase AmpC with an inhibition constant (K_i) value of 27 nM. In the crystal structure of the AmpC/**1** complex,[12] the inhibitor forms a transient covalent bond between its boronic acid moiety and the catalytic nucleophile Ser64, acting as a transition-state analog. The benzothiophene ring of the inhibitor complements the region of AmpC that would
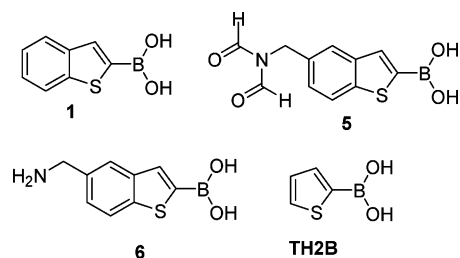
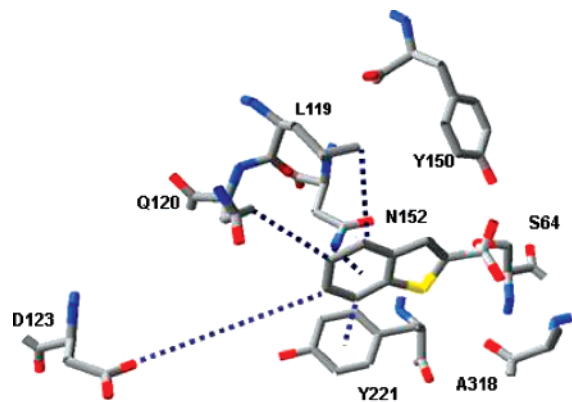**Figure 1.** Characteristic boronic acid-based β-lactamase inhibitors discussed here.

Figure 2. Interactions between compound **1** and enzyme residues in the active site of AmpC-β lactamase. Dashed lines indicate distances between aryl ring carbons and residues. C4 is 4.0 Å from Leu119, C5 is 3.7 Å from Gln120, C6 is almost 8 Å away from Asp123, and C7 is 4 Å from the centroid of Tyr221. This picture was generated using Swiss-PdbViewer.

typically recognize the R1-amide side chain of β-lactam substrates, accepting a hydrogen bond from the completely conserved Asn152 to the electron-rich benzothiophene ring (Figure 2). This unusual interaction appears to be important to the potency of this inhibitor-analogs that replace this ring system with less electron-rich analogs lose up to three log-orders of affinity, and boronic acid itself is 100 000-fold weaker as an inhibitor compared to the benzothiophene derivative. That said,

---

* To whom correspondence should be addressed. Phone: +390592055134. Fax: +390592055131. E-mail: costimp@unimore.it.
† Dipartimento di Scienze Farmaceutiche, Università degli Studi di Modena e Reggio Emilia.
‡ University of California, San Francisco.
§ Università degli Studi de L'Aquila.
‖ Dipartimento di Chimica, Università degli Studi di Modena e Reggio Emilia.

it is clear from the structure that there is room for further derivatization of the benzothiophene ring (PDB entry 1CB3).[12]

There is call for such derivitization: despite its tight binding and a ligand efficiency of 0.87, the efficacy of compound **1** on cells is modest. In combination with third generation cephalosporins like ceftazidime (CAZ[a]), the inhibitor was only active in the tens-of-micromolar range in antimicrobial cell-based assays, 1000-fold worse than its K_i value. This is a common problem for agents targeting Gram negative pathogens, whose outer membrane presents an important barrier to cell entry.[11,12]

We reasoned that improving the cellular efficacy of compound **1** demanded improvement of its solubility (clogD of 3.39, Table 1) and its ability to cross the outer membrane of Gram negative bacteria. Both the simplicity of the inhibitor and its crystallographic structure with AmpC suggested that a wide range of derivatives were possible. We used the structure of the AmpC/**1** complex to design derivatives with different physical properties that would at the same time be accommodated by the enzyme active site. We focused on derivatives at the distal C5 position of the benzothiophene ring, which were synthetically accessible and, based on model-building, appeared to fit the site well. Subsequent X-ray crystallography on one of these derivatives, compound **5**, in complex with the enzyme, confirmed that these derivatives were accommodated as designed. Overall, 24 derivates at this position were synthesized and tested for efficacy against both enzyme and whole cells. In an effort to understand the relationship between these two efficacy measurements, we developed a structure−permeability relationship, calculating physiochemical properties such as lipophilicity (LogP, LogD) and measuring ligand permeability on an immobilized artificial membrane (IAM.PC; Logk$^I_{IAM}$) column. This ultimately led to compounds with substantially higher solubility and cellular efficacy compared to compound **1**, despite affinities that were little improved, and in fact often reduced, for the pure enzyme. We consider the implications of these results for further optimization of this series of compounds and for the role of physiochemical and pharmacokinetic optimization of ligands in antimicrobial design.

Experimental Methods

Synthesis. 5-Methylbenzo[*b*]thiophene (5-MeBTH) and benzo-[*b*]thiophene-2-ylboronic acid were purchased from Lancaster. All reagents were purchased from Aldrich, Sigma, and Fluka and were of reagent grade. Reaction progress was monitored by TLC on precoated silica gel 60 F$_{254}$ plates (Merck). Silica gel (60 M; 230−400 mesh, ASTM) was used for column chromatography. The purity of all synthesized compounds was determined by elemental analyses performed on a Perkin-Elmer 240C instrument, and all values were within ±0.4% of the theoretical values. Yields refer to purified products and were not optimized. All compounds were characterized by ^{1}H NMR on AC200 and Bruker MX400 WB instruments (CIGS, University of Modena e Reggio Emilia). Some compounds were also characterized through 2D NMR and ^{13}C NMR. Unless otherwise stated, spectra were recorded in DMSO-d_6 or CDCl$_3$. Chemicals shifts are reported in ppm from tetramethylsilane as an internal standard.

Pinacol Benzo[*b*]thiophen-2-ylboronate (1a). To a solution of 0.30 g (1.68 mmol) of benzo[*b*]thiophen-2-ylboronic acid (**1**) in dry Et$_2$O (40 mL) was added pinacol (0.199 g, 1.68 mmol), and the mixture was stirred under nitrogen for 15 min. Thereafter, the reaction was treated with a catalytic amount of TFA and stirred

under nitrogen for another hour. The Et$_2$O was removed in vacuum and crude residue was extracted with pentane, affording **1a**. Yield: 0.381 g, 87%. ^{1}H NMR (DMSO): δ 1.31 (s, 12H), 7.42 (m, 2H), 7.91 (s, 1H), 7.95 (m, 1H), 8.02 (m, 1H). Anal. (C$_{14}$H$_{17}$BO$_2$S) C, H.

5-Methyl-benzo[*b*]thiophen-2-ylboronic Acid (2). *n*-BuLi (14 mmol of a 2.5 M solution in hexane) was added dropwise to a stirred solution of 5-MeBTH (1.4 g, 9 mmol) in dry THF (20 mL) at −60 °C under argon. After 75 min, a solution of tri-isopropyl-borate (3.3 mL, 14 mmol) was added, and the mixture was stirred for 15 min at −78 °C; the temperature was slowly warmed to RT and stirred for an additional hour. The mixture was then quenched with 10% HCl. The reaction mixture was extracted with Et$_2$O, and the product was precipitated as the sodium salt by the addition of 25% NaOH solution. This precipitate was dissolved in 10 mL of hot water and reprecipitated with 10% HCl affording **2** as a white crystalline solid. Yield: 1.5 g, 83%; mp 254−257 °C. ^{1}H NMR (DMSO): δ 2.41 (s, 3H), 7.19 (d, 1H), 7.69 (d, 1H), 7.82 (m, 2H), 8.37 (br s, 2H). Anal. (C$_9$H$_9$BO$_2$S) C, H.

Pinacol 5-Methylbenzo[*b*]thiophen-2-ylboronate (2a). To 1.35 g (7 mmol) of **2** in dry Et$_2$O (40 mL) was added pinacol (0.83 g, 7 mmol) and a catalytic amount of TFA. The mixture was stirred under nitrogen for 1 h. After this time the solvent was removed under vacuum and crude residue extracted with *n*-pentane, affording **2a**. Yield: 1.8 g, 94%; mp 68−70 °C. ^{1}H NMR (DMSO): δ 1.31 (s, 12H), 2.41 (s, 3H), 7.25 (dd, 1H), 7.73 (s, 1H), 7.81 (s, 1H), 7.87 (d, 1H). ^{13}C NMR (CDCl$_3$): δ 21.9, 25.7, 85.0, 122.8, 124.8, 128, 134.4, 134.8, 141.6, 141.8 (quaternary *C*B not seen). Anal. (C$_{15}$H$_{19}$BO$_2$S) C, H.
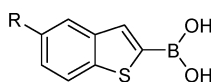
Pinacol 5-Bromomethylbenzo[*b*]thiophen-2-ylboronate (3). *N*-Bromosuccinimide (1.04 g, 6 mmol) was added to 1.6 g (6 mmol) of **2a** in CCl$_4$ (40 mL). The mixture was heated under reflux, irradiated with a UV lamp, and then benzoyl peroxide (0.124 g, 0.58 mmol) was added. The mixture was cooled with ice, and the resulting precipitate (succinimide) was removed by filtration. Filtrate was concentrated under vacuum and the crude residue was crystallized several times from hexane, affording **3** as violet solid. Yield: 1.27 g, 62%; mp 87−90 °C. ^{1}H NMR (DMSO): δ 1.39 (s, 12H), 4.65 (d, 2H), 7.42 (dd, 1H), 7.88 (m, 3H). Anal. (C$_{15}$H$_{18}$-BBrO$_2$S) C, H.

5-Hydroxymethylbenzo[*b*]thiophen-2-ylboronic Acid (4). A solution of **3** (80 mg, 0.230 mmol) in acetone/H$_2$O 1:1 (4 mL) and KI (8 mg, 10%) as catalyst was refluxed under stirring for 1 h. After this time the solvent was evaporated, and water and Et$_2$O were added. The organic layer was separated, dried (Na$_2$SO$_4$), and concentrated, affording a crude product, which was purified by crystallization from CH$_2$Cl$_2$/hexane, affording **4**. Yield: 0.039 g, 80%; mp 180−184 °C. ^{1}H NMR (DMSO): δ 4.60 (d, 2H), 5.19 (t, 1H), 7.32 (dd, 1H), 7.80 (s, 1H), 7.89 (d, 1H), 7.90 (s, 1H), 8.49 (d, 2H). Anal. (C$_9$H$_9$BO$_3$S) C, H.

Pinacol 5-Diformylaminomethylbenzo[*b*]thiophen-2-ylboronate (5). Sodium diformylamide (48 mg, 0.50 mmol) was added to a solution of **3** (0.150 g, 0.42 mmol) in CH$_3$CN (10 mL), and the mixture was heated for 7 h under reflux. The cooled mixture was filtered and washed with CH$_3$CN. The combined filtrate was concentrated under reduced pressure. Crystallization of the crude product from CH$_2$Cl$_2$/pentane afforded **5**. Yield: 0.104 g, 75%; mp 125−128 °C. ^{1}H NMR (DMSO): δ 1.38 (s, 12H), 4.91 (s, 2H), 7.41 (dd, 1H), 7.88 (m, 3H), 8.91 (br s, 2H). ^{13}C NMR (CDCl$_3$): δ 21.9, 25.7, 85.0, 122.8, 124.8, 128, 134.4, 134.8, 141.6, 141.8 (quaternary CB not seen). Anal. (C$_{17}$H$_{20}$BNO$_4$S) C, H, N.
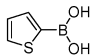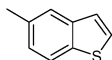
Pinacol 5-Aminomethylbenzo[*b*]thiophen-2-ylboronate (6). A mixture of **5** (0.110 g, 0.3 mmol) and 5% ethanolic HCl (2 mL, freshly prepared from 37% HCl and EtOH) was refluxed for 3 h and then evaporated under reduced pressure to near dryness. The crude product was washed with Et$_2$O, affording **6** as crystalline solid. Yield: 0.080 g, 77%; mp > 220 °C. ^{1}H NMR (DMSO): δ 1.31 (s, 12H), 4.15 (s, 2H), 7.55 (dd, 1H), 7.92 (s, 1H), 8.03 (s, 1H), 8.08 (d, 1H), 8.38 (br s, 2H). ^{13}C NMR (DMSO): δ 24.4, 42.1, 84.3, 122.7, 124.9, 126.4, 130.2, 134.2, 139.9, 142.6 (quaternary *C*B not seen). Anal. (C$_{15}$H$_{20}$BNO$_2$S) C, H, N.

Table 1. Summary Table of K_i and Molecular Properties

Code	Structure of R	$K_i{}^a$ (μM)	clogP	clogD[b,c]	clogD[e,d]	logk[I][IAM]	pKa[e]
1	—H	0.027	3.75(±0.79)	3.39	3.75	1.19, 1.16[g]	6.39[h]
2	—CH₃	0.030	4.21(±0.79)	3.89	4.21	1.54	6.39[h]
3	—Br	0.03–0.05	4.45(±0.80)	4.02	4.45	0.74[g]	6.39[h]
4	—OH	0.043	2.57(±0.80)	2.21	2.57	-0.36	6.39[h]
5	(N,N-diformyl ethyl)	0.037	2.42(±0.80)	1.79	2.42	-	6.39[h], -1.45[i]
6	—NH₂	0.260	2.62(±0.81)	0.53	-0.48	-0.02[g]	9.26[i], 6.39[h]
7	(N-formyl ethylamino)	0.45	2.71(±0.81)	2.12	2.71	-	15.57[i], 6.39[h] 0.64[i]
8	(3-nitrophenylaminoethyl)	0.037	5.05(±0.82)	4.51	4.98	0.23	6.39[h], 2.20[i]
9	(4-(hexafluoro-2-hydroxyisopropyl)phenylaminoethyl)	0.028	4.88(±1.13)	5.69	6.18	0.74[g]	6.39[h], 2.93[i]
10	(3,4-dichlorophenylaminoethyl)	0.010	6.35(±0.89)	5.80	6.28	0.98[g]	6.39[h], 2.25[i]
11	(phenoxyethyl)	0.250	5.32(0.80)	4.93	5.32	-	6.39[h]
12	(3,4-dichlorophenoxyethyl)	0.083	6.71(±0.82)	6.30	6.71	-	6.39[h]
13	(benzyloxyethyl)	0.600	5.48(±0.83)	4.93	5.32	-0.20[g]	6.39[h]
14	(phenylthioethyl)	0.080	5.33(±0.88)	4.94	5.33	-0.18[g]	6.39[h]
15	(3,4-dimethoxyphenylaminoethyl)	0.250	4.10(±0.82)	3.57	2.85	-	6.39[h], 4.25[i]
16	(N,N-bis(2-hydroxyethyl)aminoethyl)	1	3.01(±0.89)	2.24	-0.056	-	15.04[l], 14.36[l] 6.39[h], 6.77[i]
17	(piperazinylethyl)	2	2.89(±0.88)	0.71	-0.64	-	6.39[h], 9.30[i] 3.37[i]
18	(3-boronophenylaminoethyl)	0.045	4.03(±1.11)	3.47	3.21	-	6.39[h], 3.76[i]
19	(4-acetylphenylaminoethyl)	0.250	4.54(±0.82)	4.00	4.54	0.88	6.39[h], 0.85[i]
20	(3-carboxyphenylaminoethyl)	nt[f]	4.69(±0.82)	1.35	4.32	-	6.39[h], 4.32[m] 2.94[i]
21	(4-morpholinophenylaminoethyl)	0.800	3.83(±0.84)	3.29	1.50	0.88[g]	6.39[h], 5.77[i] -0.24[i]
22	(N-(carboxymethyl)aminoethyl)	0.028	2.65 (±0.84)	-0.31	0.11	-	9.13[i], 6.39[h] 2.20[m]
23	(imidazolylethyl)	0.082	2.99(±0.88)	2.35	0.52	-	6.39[h], 6.75[i]
24	(3-amino-1,2,4-triazolium ethyl)	0.170	2.27(±0.89)	1.53	1.71	0.06	6.39[h], 3.65[i] -2.71[i]

Table 1. Continued

Code	Structure	Ki (μM) [a]	clogP	clogD[b,c]	clogD[e,d]	logk[I][IAM]	pKa[e]
TH2B		2.5	1.27(±0.78)	1.25	1.27	-	7.16[h]
5-MeBTH		ntf	4.84(±0.25)	4.84	4.84	-	-

[a] Estimated error margins on the K_i values are ±20%. [b] Calculated at pH 7.4. [c] Estimated error margins on the clogD values are ±0.8. [d] Calculated at pH 3. [e] Estimated error margins on the pK_a values are ±20%. [f] Not tested. [g] Values of Logk[I][IAM] calculated for pinacol ester. [h] Measured pK_a for boronic acid. [i] Calculated pK_a for N atom. [l] Calculated pK_a for O atom. [m] Calculated pK_a for carboxylic group.

5-Formylaminomethylbenzo[*b*]thiophen-2-ylboronic Acid (7). A solution of **5** (23 mg, 0.07 mmol) in methanol (1 mL) was stirred for 2 h at room temperature. Removal of the solvent under reduced pressure afforded pure **7**. Yield: 0.008 g, 51%. ^{1}H NMR (DMSO): δ 4.41 (d, 2H), 7.31 (dd, 1H), 7.75 (s, 1H), 7.91 (d, 1H), 8.14 (s, 1H) 8.42 (s, 2H), 8.50 (br s, 1H). Anal. ($C_{10}H_{10}BNO_3S$) C, H, N.

General Procedure for the Synthesis of Amino Derivatives 8–10 and 15–21. A mixture of **3** (0.070–0.150 g, 0.20–0.42 mmol), an appropriate amine (1.1–1.5 equiv), and 1.1 equiv of NaHCO₃ or Na₂CO₃ was stirred in dry DMF (2–4 mL) at 80 °C for 4–24 h. On reaction termination, the mixture was cooled and poured into water, and the resulting precipitate was separated by filtration. The filtrate was extracted several times with ethyl acetate or chloroform. The combined organic phases were dried over Na₂SO₄ and evaporated under reduced pressure to give crude product, which were then purified by chromatography or crystallization.

General Procedure for the Synthesis of Ether Derivatives 11–13. Phenate (1 equiv, freshly prepared from an appropriate phenol and sodium in ethanol) was added to a solution of **3** and a catalytic amount of KI in dry DMF (2.5 mL). The mixture was stirred at 60 °C until starting material disappeared on TLC and then extracted with Et₂O or CH₂Cl₂ (3 × 10 mL). The organic layer was dried over Na₂SO₄ and evaporated, and the crude residue was purified by silica gel chromatography and by crystallization.

Pinacol 5-[(3-Nitrophenylamino)methyl]benzo[*b*]thiophen-2-ylboronate (8). Compound **8** was prepared starting from **3** (0.150 g, 0.42 mmol) and 3-nitroaniline (0.087 g, 0.63 mmol). The crude residue was purified by crystallization from CH₂Cl₂/hexane. Yield: 0.050 g, 29%; mp 101–103 °C. ^{1}H NMR (DMSO): δ 1.31 (s, 12H), 4.44 (d, 2H), 6.99–7.10 (m, 2H), 7.25–7.49 (m, 4H), 7.87–8.10 (m, 3H). Anal. ($C_{21}H_{23}BN_2O_4S$) C, H, N.

5-[(3-Nitrophenylamino)methyl]benzo[*b*]thiophen-2-ylboronic Acid (8-bis). Compound **8-bis** was prepared starting from **3** (0.150 g, 0.42 mmol) and 3-nitroaniline (0.087 g, 0.63 mmol). The crude residue was purified by crystallization from MeOH/H₂O, affording the free boronic acid of **8**. Yield: 0.020 g, 12%. ^{1}H NMR (DMSO): δ 4.46 (d, 2H), 6.99–7.10 (m, 2H), 7.29–7.41 (m, 4H), 7.87–7.92 (m, 3H), 8.40 (s, 2H). Anal. ($C_{15}H_{13}BN_2O_4S$) C, H, N.

Pinacol 5-{[4-(1-Hydroxy-2,2,2-trifluoro-1-trifluoromethylethyl)-phenylamino]methyl}benzo[*b*]thiophen-2-ylboronate (9). Compound **9** was prepared from **3** (0.080 g, 0.23 mmol) and 2-(4-aminophenyl)-1,1,1,3,3,3-hexafluoro-2-propoanol (0.090 g, 0.34 mmol). The crude product was purified by column chromatography using CHCl₃/CH₃OH 9:1 as an eluent and for final purification by crystallization from acetone/petroleum ether. Yield: 0.030 g, 25%. ^{1}H NMR (DMSO): δ 1.32 (s, 12H), 4.42 (d, 2H), 6.66 (d, 2H), 7.31 (d, 2H), 7.45 (dd, 1H), 7.87 (s, 1H), 7.93 (s, 1H), 7.97 (d, 1H). Anal. ($C_{24}H_{24}BF_6NO_3S$) C, H, N.

Pinacol 5-[(3,4-Dichlorophenylamino)methyl]benzo[*b*]thiophen-2-ylboronate (10). Compound **10** was prepared starting from **3** (0.150 g, 0.42 mmol) and 3,4-dichloroaniline (0.102 g, 0.63 mmol). The crude product was purified by fractional crystallization from CH₂Cl₂/hexane. Yield: 0.052 g, 28%; mp 164–167 °C. ^{1}H NMR (DMSO): δ 1.31 (s, 12H), 4.39 (d, 2H), 6.58 (dd, 1H), 6.76 (d,

1H), 6.7–6.8 (br s/o, 1H), 7.21 (d, 1H), 7.42 (dd, 1H), 7.87 (s, 1H), 7.90 (s, 1H), 7.97 (d, 1H). Anal. ($C_{21}H_{22}BCl_2NO_2S$) C, H, N.

Pinacol 5-Phenoxymethylbenzo[*b*]thiophen-2-ylboronate (11). Compound **11** was prepared from **3** (0.095 g, 0.27 mmol) and sodium phenoate. The crude product was purified by crystallization from CH₂Cl₂/hexane. Yield: 0.050 g, 51%. ^{1}H NMR (DMSO): δ 1.4 (s, 12H), 4.4 (s, 2H), 7.1–7.6 (m, 6H), 7.7–7.9 (m, 3H). Anal. ($C_{21}H_{23}BO_3S$) C, H.

Pinacol 5-(3,4-Dichlorophenoxymethyl)benzo[*b*]thiophen-2-ylboronate (12). Compound **12** was prepared from **3** (0.150 g, 0.42 mmol) and sodium 3,4-dichlorophenoate. The crude product was purified by column chromatography using CHCl₃/EtOAc 5:5 as eluent. Yield: 0.020 g, 11%. ^{1}H NMR (DMSO): δ 1.3 (s, 12H), 4.3 (s, 2H), 7.1–7.6 (m, 6H), 7.8–8.0 (m, 3H). Anal. ($C_{21}H_{21}$-BCl_2O_3S) C, H.

Pinacol 5-Benzyloxymethylbenzo[*b*]thiophen-2-ylboronate (13). Compound **13** was prepared from **3** (0.110 g, 0.31 mmol) and sodium benzylate. The crude residue was purified by column chromatography using CHCl₃/EtOAc 5:5 as eluent. Crystallization of this residue from CH₂Cl₂/hexane gave **13**. Yield: 50%. ^{1}H NMR (DMSO): δ 1.31 (s, 12H), 4.57 (s, 2H), 4.66 (s, 2H), 7.35 (m, 5H), 7.43 (dd, 1H), 7.91 (s, 1H), 7.95 (s, 1H), 8.10 (d, 1H). Anal. ($C_{22}H_{25}BO_3S$) C, H.

Pinacol 5-Phenylsulphanylmethylbenzo[*b*]thiophen-2-ylboronate (14). A mixture of **3** (0.060 g, 0.17 mmol), thiophenol (27 μL, 0.25 mmol), and 1.1 equiv of NaHCO₃ was stirred at 60 °C in dry DMF for 24 h. The mixture was cooled and extracted with Et₂O; the organic layer was dried over Na₂SO₄ and evaporated under reduced pressure, affording **14**. Yield: 0.030 g, 46%; mp 121–124 °C. ^{1}H NMR (DMSO): δ 1.31 (s, 12H), 4.34 (s, 2H), 7.12–7.15 (m, 6H), 7.85 (s, 1H), 8.00 (s, 1H), 8.20 (d, 1H). Anal. ($C_{21}H_{23}BO_2S_2$) C, H.

Pinacol 5-[(3,4-Dimethoxyphenylamino)methyl]benzo[*b*]thiophen-2-ylboronate (15). Compound **15** was prepared following the general method, as described above, from **3** (0.070 g, 0.20 mmol) and 3,4-dimethoxyaniline (0.152 g, 0.99 mmol). The crude product was purified by column chromatography using CHCl₃/EtOAc 9:1 as eluent. Yield: 0.017 g, 20%. ^{1}H NMR (DMSO): δ 1.31 (s, 12H), 3.54 (s, 3H), 3.64 (s, 3H), 4.31 (s, 2H), 6.04 (dd, 1H), 6.35 (d, 1H), 6.65 (d, 1H), 7.42 (dd, 1H), 7.90 (m, 3H). Anal. ($C_{23}H_{28}BNO_4S$) C, H, N.

Pinacol 5-{[Bis(2-hydroxyethyl)amino]methyl}benzo[*b*]thiophen-2-ylboronate (16). Compound **16** was prepared from **3** (0.080 g, 0.23 mmol) and diethanolamine (0.121 g, 1.15 mmol). The aqueous phase was concentrated and the crude product was crystallized from CH₃OH/EtOAc. Yield: 0.021 g, 24%. ^{1}H NMR (DMSO): δ 1.31 (s, 12H), 2.55 (t, 4H), 3.63 (m, 4H), 3.73 (s, 2H), 7.5 (dd, 1H), 7.70–7.80 (m, 3H). Anal. ($C_{19}H_{28}BNO_4S$) C, H, N.

Pinacol 5-Piperazin-1-ylmethylbenzo[*b*]thiophen-2-ylboronate (17). Compound **17** was prepared following the general method, as described above, starting from **3** (0.150 g, 0.42 mmol) and piperazine (0.073 g, 0.85 mmol). The crude residue was washed with Et₂O to give a gray crystalline solid **17**. Yield: 0.030 g, 20%. ^{1}H NMR (DMSO): δ 1.41 (s, 12H), 2.32 (m, 4H), 2.69 (m, 4H),
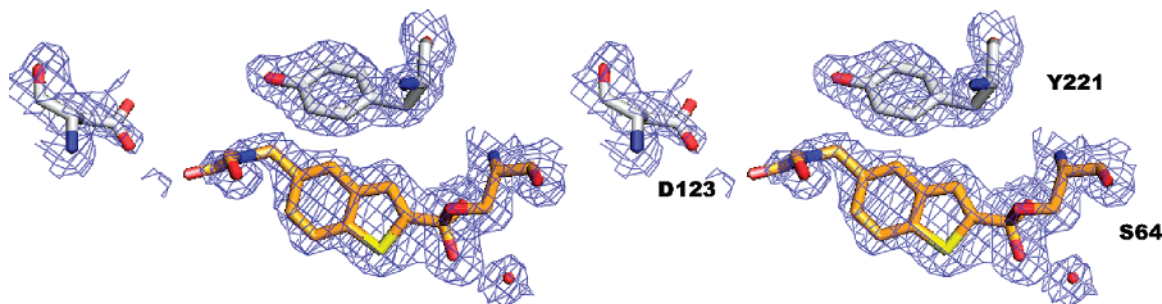
Figure 3. Stereoview of electron density of compound **5** in complex with AmpC. The 2*Fo*−*F*c electron density map is represented by the blue cage and is contoured at 1.0σ. Carbon atoms of AmpC, gray; carbon atoms of **5**, orange; nitrogen atoms, blue; oxygen atoms, red; and sulfur atoms, yellow. This picture was generated using Pymol (www.pymol.com).

3.51 (s, 2H), 7.35 (dd, 1H), 7.80−8.00 (m, 3H). Anal. ($C_{19}H_{27}$-BN_2O_2S) C, H, N.

Pinacol 5-[(Phenylamino3-boronicacid)methyl]benzo[*b*]thiophen-2-ylboronate (18). Compound **18** was prepared following the general method, as described above, starting from **3** (0.05 g, 0.14 mmol) and 3-aminophenylboronic acid (0.052 g, 0.28 mmol). The crude residue was washed with Et_2O, affording **18**. Yield: 0.005 g, 7%. ^{1}H NMR (DMSO): δ 1.3 (s, 12 H), 4.8 (s, 2H), 7.0 (m, 1H), 7.4 (d, 2H), 7.6−8.1 (m, 5H), 8.4 (s br, 2H). Anal. ($C_{21}H_{25}B_2NO_4S$) C, H, N.

Pinacol 5-[(4-Acetylphenylamino)methyl]benzo[*b*]thiophen-2-ylboronate (19). Compound **19** was prepared following the general method, as described above, starting from **3** (0.120 g, 0.34 mmol) and 4-aminoacetophenone (0,138 g, 1 mmol). The crude product was purified first by crystallization from EtOAc/hexane and by crystallization from acetone/petroleum ether, subsequently. Yield: 0.028 g, 20%. ^{1}H NMR (DMSO): δ 1.32 (s, 12H), 2.36 (s, 3H), 4.47 (s, 2H), 6.63 (dd, 2H), 7.43 (dd, 1H), 7.68 (d, 2H), 7.92 (m, 3H). Anal. ($C_{23}H_{26}BNO_3S$) C, H, N.

Pinacol 5-[(3-Carboxyphenylamino)methyl]benzo[*b*]thiophen-2-ylboronate (20). Compound **21** was prepared following the general method, as described above, from **6** (0.080 g, 0.23 mmol) and 3-aminobenzoic acid (0.158 g, 1.15 mmol). The crude product was purified by crystallization from acetone/petroleum ether. Yield: 0.021 g, 22% ^{1}H NMR (DMSO): δ 1.31 (s, 12H), 4.32 (d, 2H), 6.7−6.8 (m, 2H), 7.1−7.2 (m, 6H), 12 (s br., 1H). Anal. ($C_{22}H_{24}BNO_4S$) C, H, N.

Pinacol 5-[(4-Morpholin-4-yl-phenylamino)methyl]benzo[*b*]-thiophen-2-ylboronate (21). Compound **21** was prepared following the general method, as described above, from **3** (0.070 g, 0.20 mmol) and 4-morpholin-4-yl-aniline (0.177 g, 0.99 mmol). The crude product was purified by column chromatography using $CHCl_3$/EtOAc 5:5 as eluent. Yield: 0.015 g, 17%. ^{1}H NMR (DMSO): δ 1.32 (s, 12H), 2.86 (m, 4H), 3.68 (m, 4H), 4.32 s, 2H), 5.85 (br s, 1H), 6.55 (m, 2H), 6.72 (m, 2H), 7.42 (dd, 1H), 7.85−7.96 (m, 3H). Anal. ($C_{25}H_{31}BN_2O_3S$) C, H, N.

Pinacol 5-[(Carboxymethylamino)methyl]benzo[*b*]thiophen-2-ylboronate (22). A mixture of **3** (0.10 g, 0.28 mmol), glycine (0.021 g, 0.28 mmol), and 2,6-lutidin (65 μL, 0.56 mmol) in dry DMF (2.5 mL) was stirred for 17 h at 80 °C. The mixture was cooled and poured into water, and the resulting precipitate separated by filtration. The filtrate was extracted with ethyl acetate, and the organic phase was dried (Na_2SO_4) and then evaporated under reduced pressure to give **22** as a yellow oil. Yield: 0.030 g, 30%; mp > 300 °C. ^{1}H NMR (DMSO): δ 1.31 (s, 12H), 4.61 (d, 2H), 5.25 (t, 1H), 7.38 (dd, 1H), 7.92 (m, 2H). Anal. ($C_{17}H_{22}BNO_4S$) C, H, N.

5-Imidazol-1-yl-methylbenzo[*b*]thiophen-2-ylboronic Acid (23). A 20% dispersion of NaH in mineral oil (5.6 mg, 0.187 mmol) was added portionwise to a stirred solution of imidazole (11.6 mg, 0.170 mmol) in dry DMF. The mixture was stirred for 1 h and then was added a solution of **3** (60 mg, 0.170 mmol) in dry DMF. The mixture was stirred at room temperature for 15 h and then poured into water. Extraction with EtOAc gave a solid that was crystallized from EtOAc/petroleum ether. Yield: 0.012 g, 21%;

mp 140−144 °C. ^{1}H NMR (DMSO): δ 1.31 (s, 12H), 5.32 (s, 2H), 6.94 (s, 1H), 7.21 (s, 1H), 7.29 (dd, 1H), 7.73 (s, 1H), 7.78 (s, 1H), 7.89 (s, 1H), 7.98 (d, 1H). Anal. ($C_{12}H_{11}BN_2O_2S$) C, H, N.

5 [(1,2,4-Triazol-1-ylmethyl]benzo[*b*]thiophen-2-ylboronic Acid (24). A mixture of **3** (150 mg, 0.42 mmol), 4-amino-1,2,4-triazole (0.036 g, 0.42 mmol), and 2,6-lutidin (99 μL, 0.85 mmol) in dry DMF (2.5 mL) was stirred for 2 h at 80 °C. Removal of the solvent under reduced pressure gave an orange oil that was washed with CH_2Cl_2, affording **24**. Yield: 0.037 g, 33%; mp 152−156 °C. ^{1}H NMR (DMSO): δ 5.70 (s, 2H), 6.94 (br s, 2H), 7.43 (dd, 1H), 7.96 (s, 1H), 8.00 (s, 1H), 8.02 (d, 1H), 8.48 (br s, 2H), 9.17 (s, 1H), 10.34 (s, 1H). ^{13}C NMR (DMSO): δ 55.5, 123.5, 125.4, 125.7, 129.7, 132.9, 141.2, 143.1, 143.6, 146 (quaternary *C*B not seen). ^{15}N NMR (DMSO): δ −81,0−152,0−181,0−297.3. Anal. ($C_{11}H_{12}$-BN_4O_2S) C, H, N.

Crystal Growth and Structure Determination. Cocrystals of AmpC in complex with compound **5** were grown by vapor diffusion in hanging drops equilibrated over 1.8 M potassium phosphate buffer, pH 8.7, using microseeding. The initial concentration of the protein in the drop was 3.8 mg/mL, and the concentration of the compound was 0.8 mM. The compound was added to the crystallization drops in a solution of 1.2% DMSO, 1 M potassium phosphate buffer, pH 8.7. Crystals appeared after equilibrating for several weeks at 21 °C. Before data collection, crystals were immersed in a cryoprotectant solution of 20% sucrose, 1.8 M potassium phosphate, pH 8.7, for about 30 s, and were then flash-cooled in liquid nitrogen. Diffraction data were collected on frozen crystals at the Advance Light Source (ALS, Lawrence Berkeley Laboratory, California). Reflections were indexed, integrated, and scaled using the HKL software package and MOSFLM.[15,16] The space group was *C*2, with two molecules in the asymmetric unit. Molecule 1 of the asymmetric unit was modeled with 357 residues, including the inhibitor, whereas molecule 2 was modeled with 346 residues, including the inhibitor (11 residues, 283−293 were left out due to poor density in this region, which is often disordered in AmpC structures). The initial phasing model was the binary complex of AmpC/**1** with inhibitor, water molecules, and ions removed (PDB entry 1CB3).[12] The models were positioned using rigid body refinement and refined using the maximum likelihood target in CNS, including simulated annealing, positional minimization, and individual *B*-factor refinement, with a bulk solvent correction.[17] Sigma A-weighted electron density maps were calculated using CNS and used in further steps of manual model rebuilding and placement of water molecules with the programs XtalView[18] (Figure 3). The inhibitor was built into the 2*Fo*−*F*c and *Fo*−*F*c electron density maps in each active site of the asymmetric unit. Subsequent refinement cycles involved positional minimization and B-factor refinement in CNS (Table 2).

Data Deposition. The coordinates and structure factors have been deposited in the Protein Data Bank under accession codes PDB ID 2I72, RCSB ID RCSB039218.

Enzymology. Boronic acids were dissolved in DMSO at a concentration of 1−100 mM; more dilute stocks were subsequently prepared as necessary. Compounds isolated as pinacol-protected boronic acid were tested without further ester cleavage reaction;

Table 2. Data Collection and Refinement Statistic

	AmpC/5
cell constants	
a (Å)	117.191
b (Å)	76.756
c (Å)	97.52
β (deg)	116.718
space group	$C2$
resolution (Å)	2.05 (2.16−2.05)[a]
unique reflections	48.125
total observations	179.888
Rmerge (%)	10.3 (51.2)[a]
completeness[b] (%)	98.0 (96.8)[a]
resolution range for refinement (Å)	20−2.05
$<I>/<\sigma 1>$	13.5 (2.7)[a]
number of protein residues	705
number of water molecules	430
RMSD bond lengths (Å)	0.0061
RMSD bond angles (°)	1.33
Rcryst (%)	20.13
Rfree (%)[c]	24.74
avg B factor, protein atoms (Å^2, molecule 1,2)	23.40
avg B factor, inhibitor atoms (Å^2, molecule 1)	34.20
avg B factor, inhibitor atoms (Å^2, molecule 2)	32.26
avg B factor, Å^2 water molecules	34.22

[a] Highest resolution shell in parentheses. Subsequent values in parentheses are for that shell. [b] Fraction of theoretically possible reflections observed. [c] Rfree was calculated with 5% of reflections, randomly selected, set aside.

compounds were hydrolyzed to the free acids by dissolving them in 50 mM phosphate buffer at pH 7.4.[14] Kinetic measurements were performed using 100 μM of cephalothin (sodium salt, Sigma) as a substrate in 50 mM potassium phosphate buffer, pH 7.4, and monitored at 265 nm, 25 °C, on an HP8543 UV/Visible spectrophotometer. The concentration of AmpC was determined spectrophotometrically in concentrated stock solutions made from lyophilized powder and subsequently diluted; this enzyme had been previously expressed and purified, as described.[12] The concentration of enzyme in all reactions was 1.5 nM. K_i values were obtained from IC$_{50}$ plots assuming competitive inhibition, using a K_m of cefalothin of 40 μM.[11] The background rate of cephalothin hydrolysis was found to be negligible under these conditions (approximately 1%) and was not corrected for our analyses. The effect of DMSO on enzyme activity was negligible. All experiments were repeated at least three times and the standard error was within the 20%.

Microbiology. Ampicillin and ceftazidime were obtained from Sigma Chemical Co. (St. Louis, Mo) and Glaxo Wellcome (Verona, Italy), respectively. 5-MeBTH and benzo[*b*]thiophen-2-ylboronic acid were purchased from Lancaster.

Bacterial strains: a lab strain of *E. coli* K12 JM109 that overexpresses AmpC under control of a heat-sensitive pOGO plasmid[19] was used. *E. coli* DH5alfa/pAD7, which overexpresses AmpC β-lactamase, was a gift from Prof. Moreno Galleni, University of Liege, Belgium. *E coli* DH5alfa (Life Technologies, Milan, Italy) was used as control.

Susceptibility Testing against *Escherichia coli* K12 JM109. Antibiotic susceptibility was performed and interpreted following the guidelines of the National Committee for Clinical Laboratory Standards.[20] To test their inhibitory activity, compounds were dissolved in 50% DMSO and diluted into growth medium. In all measurements of minimum inhibitory concentrations (MICs), the concentration of DMSO was always below 5%. The MIC of the β-lactams ampicillin, in the presence and absence of the boronic acids, was determined against *E. coli* K12 JM109 that express AmpC from *E. coli*.

Susceptibility Testing against *Escherichia coli* DH5α/pAD7. MICs were determined by conventional broth microdilution procedures in 0.1 mL volumes of Mueller Hinton broth. A final inoculum of 5 × 10^5 CFU/mL was used, as suggested by the Clinical Laboratory Standards Institute (CLSI).[21] The CLSI breakpoints for susceptibility, intermediate susceptibility, and resistance

was followed for ampicillin and CAZ (32 μg/mL for both). A total of 5 μL in 0.1 mL final volumes of broth at a concentration corresponding to three times K_i value for all inhibitors were used. After 16−20 h of aerobic incubation at 37 °C overnight, the trays were examined for growth. MIC results were recorded as the dilution value at which no visible growth occurred. The same microdilution procedure was used when testing inhibitors **1** and **6** at decreasing concentrations in serial 2-fold dilutions, always in the presence of CAZ: from 720 nM to 45 nM for compound **1** and from 6400 nM to 400 nM for **6**. We note that compound **1** was insoluble at concentrations below 720 nM, whereas the solubility limit of **6** was not reached even at the highest concentrations tested here.

Dissociation Constant Determination. pK_a values for reference compounds were determined spectrophotometrically using two methods. In the first method spectra were recorded at pH between 2 and 12 (ionic strength fixed at 0.01 μ). The sample concentrations in water were 10^{-4} M. All measurements spectra were recorded on spectrophotometer Cary UV 50 Varian. In the second method spectra were recorded by titrating 10^{-4} M compound solutions in water at pH 2 (HCl 0.5 N) with NaOH 0.5 N. Titrations were continued until pH 12 was reached; experiments were performed using a system probe in batch.

Data elaboration was performed using Handerson−Hasselbalch equation, absorption spectra extrapolation methods and mathematical analyses using the pHAB program.[22]

Biochromatography Separation on IAM.PC Phase. Chromatograms were obtained using a Merck Hitachi GL-6200 intelligent pump equipped with Merck Hitachi UV-detector L-7400. Merck Hitachi D-7000 HPLC software was used to record and process the chromatograms. Analyte solutions were prepared by dilution of compounds in 100 μL of DMSO and then adding CH$_3$-CN to 1 mL of volume. The concentrated stock was then diluted to a final concentration of 100 mg/mL in the mobile phase. Phosphate buffer, pH 3, was obtained by dissolving 27.6 g of NaH$_2$PO$_4$·H$_2$O in 1 L of water; pH was adjusted with concentrated H$_3$PO$_4$. The mobile phase was phosphate buffer and CH$_3$CN (75:25 v/v). Analytical HPLC IAM.PC:DD was packed into a column 10 cm and 4.6 mm I.D. The detector was set at 254 nm, the flow rate was set to 0.5 mL/min, with a 20 μL loop, and the temperature of the experiment was 25 °C.

For 5-MeBTH, **1**, **2**, **3**, and **23**, experimental determination of LogP was performed through classical shake flask and RP-LC analytical methods.[23] The experimentally determined values were compared with those predicted ones by the ACDlab software; LogP values for the remaining compounds were then calculated with this same program (Table 1). LogD values for compound **1** were first obtained from the measured LogP and the experimental pK_a value, applying the following equation

$$LogD = LogP - Log[1/(1 + 10(pH - pK_a))]$$

Results and Discussion

Structure-Based Design and Synthesis of First Round Inhibitors. Whereas compound **1** was the most potent of the original arylboronic acid inhibitors of AmpC,[11] its activity against cells did not track its affinity. Thus, the analogous thiophene-2-ylboronic acid (TH2B, Table 1) was 100-fold worse as an inhibitor of AmpC, but its activity against resistant cells was only diminished 4-fold. This suggests a barrier to cell entry for compound **1**, consistent with its poor relative solubility. Compound **1** is thought to passively diffuse through the outer membrane of Gram negative bacteria, based on its equipotent activity on cells with and without outer-membrane porin channel deletions.[12] We speculated that the better bioavailability of TH2B might reflect its lower hydrophobicity; the cLogP of this compound is 1.27 versus a cLogP of 3.75 for compound **1**.

This motivated us to explore derivatives of compound **1** that would vary in their hydrophobicity without major changes in

Scheme 1. (A) Synthesis of First Set of Derivatives of the Compound **1**; (B) in Parallel Second Set of Derivatives of Compound **1**; (C) Classical Synthesis of Second Set of Compound **1**[a]
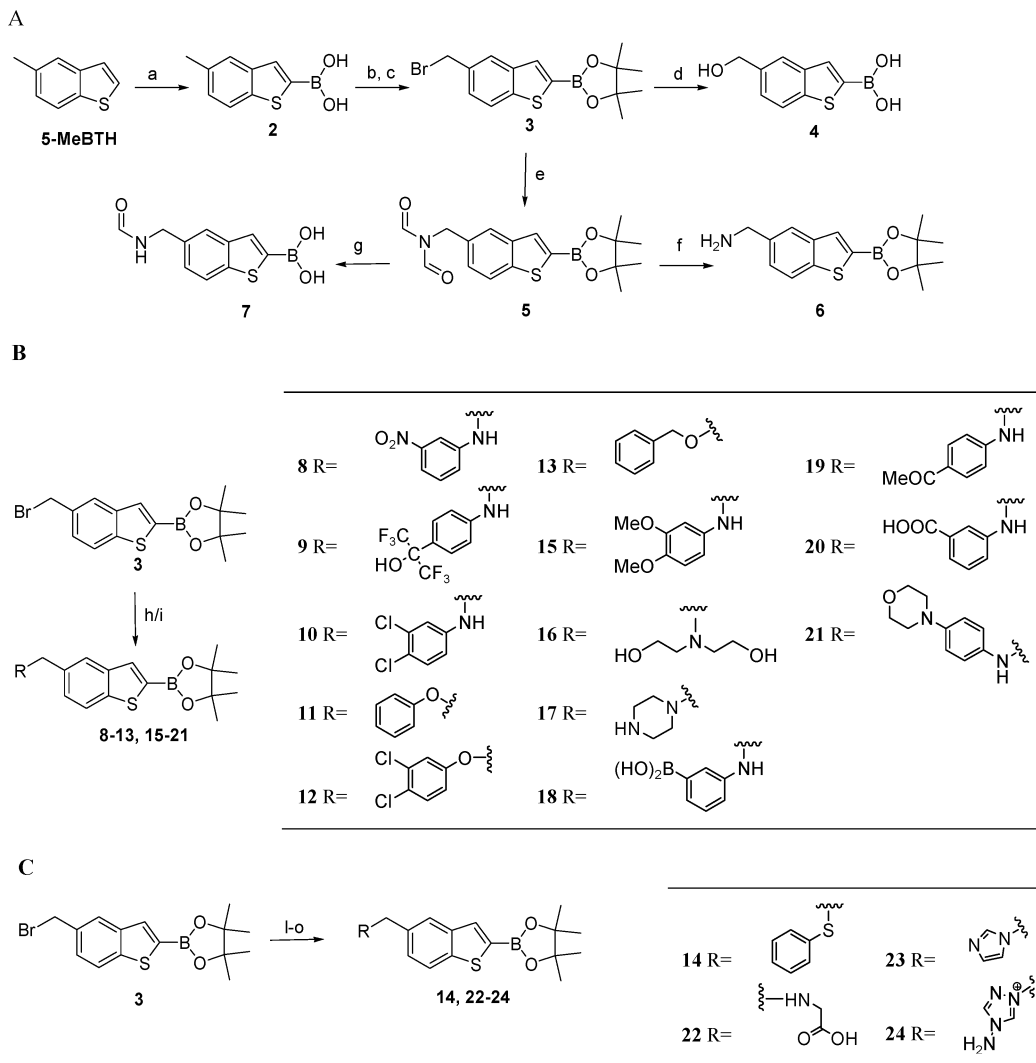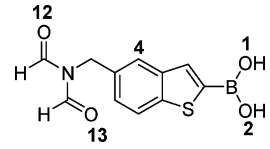

[a] Reagents and conditions: (a) *n*-BuLi, triisopropylborane, THF dry, −78 °C; (b) pinacol, Et$_2$O dry, RT; (c) NBS, benzoyl peroxide, CCl$_4$, 80 °C; (d) acetone/H$_2$O 50%, KI, reflux; (e) sodium diformylamide, CH$_3$CN, reflux; (f) 5% ethanolic HCl, reflux; (g) MeOH, RT; (h) RNH$_2$, DMF dry, NaHCO$_3$ or Na$_2$CO$_3$; (i) sodium ethylate, ROH, KI, reflux; (l) thiophenol, DMF dry, NaHCO$_3$, 60 °C; (m) glycine, 2,6-lutidin, DMF dry, 80 °C; (n) imidazole, NaH, DMF dry; (o) 4-amino-1,2,4-triazole, 2,6-lutidin, DMF dry, 80 °C.

their enzyme affinities. The most obvious point of derivatization of compound (**1**), based on the structure of the AmpC/**1** complex, was at the distal end of the benzothiophene ring, where added side chains would point out toward solvent. Whereas C6 of the benzothiophene was the least hindered of these distal sites, synthetic accessibility favored position C5. Although derivatives of **1** that maintained its exact orientation in the active site would not tolerate many substitutions at this position, we reasoned that, based on double occupancy observed in the original AmpC/**1** complex, the inhibitor could flip by 180° around its benzothiophene−boronic acid bond, exchanging C5 for C6.

A first set of derivatives of compound **1** at C5 was designed and synthesized to reduce cLogP values, introduce diversity, and introduce minimal steric hindrance.[24,25] Starting from the commercially available 5-MeBTH, the boronic group was introduced to give compound **2**, and radical bromuration afforded 5-bromomethylbenzo[*b*]thiophene-2-ylboronic acid (**3**); this compound provided a starting scaffold for structural modification (Scheme 1A). Small functional groups such as hydroxymethyl (compound **4**), diformylaminomethyl (compound **5**), aminomethyl (compound **6**), and monoformylaminomethyl

(compound **7**) were made. The K_i values against AmpC β-lactamase for compounds **2**, **3**, **4**, and **5** ranged from 30 to 43 nM, resembling that of the lead **1** (27 nM). Conversely, the K_i value for the cationic **6** increased (worsened) substantially, to 260 nM, and that for compound **7** was also much increased at 450 nM (Table 1).

X-ray Crystallography and a Second Round of Design and Synthesis. To understand the effects of these derivatives, we wanted to ensure that they were accommodated within the active site as modeled, that is, with the inhibitor maintaining essentially the same position as in the AmpC/**1** complex, moduling only a ring flip. We therefore crystallized one of the larger derivatives, the 5-diformylamino derivative compound **5**, in complex with AmpC. The structure of this complex was determined to 2.0 Å resolution by X-ray crystallography (Tables 2 and 3and Figure 3). Overall, the structure closely resembles that of the AmpC/**1** complex; as expected, the benzothiophene ring has rotated by 180° with respect to compound **1** to accommodate the diformyl group side chain. Otherwise, all interactions are essentially conserved in the two structures (Table 3 and Figure 4). The O2 atom of the boronic acid hydrogen bonds to the hydroxyl of Tyr150 and to Thr316, the latter via two well-ordered water

Table 3. Key Interactions AmpC−Compound **5**

	distance, Å	
interaction	molecule A	molecule B
Y150OH−O2	2.5	2.6
S64N−O1	2.8	2.7
A318N−O1	2.8	2.7
A318O−O1	3.0	2.9
O2−H2O	2.9 (73)	2.9 (253)
H2O−T316Oγ1	2.7	2.9
O2−H2O	3.2 (777)	
K67Nz−S64Oγ	2.7	2.7
N152Nδ2−centroid aryl ring	3.4	3.6
Y221CD2−C4 aryl ring	3.4	3.5
Q120Oε1−O12	3.4	3.0
O12−H2O	3.3 (65)	
O12−D123Oδ1		2.8
O12−H2O	3.5 (107)	
H2O−D123Oδ1	3.0	
O13−N152Nδ2		3.4
O13−V121N		3.5

molecules. The boronic acid O1 atom hydrogen bonds with the backbone nitrogens of Ser64 and Ala318 and with the carbonyl oxygen of Ala318. As in the AmpC/**1** complex, the inhibitor forms quadrupole−quadrupole interactions with Tyr221 and quadrupole−dipole interactions with Asn152 (Figure 4). The distance between ring carbon atom 7 of the inhibitor and the aromatic ring centroid of Tyr221 is 3.43 Å, and the distance between the centroid of the second ring of compound **5** and the amide nitrogen of Asn152 is 3.43 Å (Table 3).

The only substantial difference between the complexes with compounds **1** and **5** owes to the additional diformyl group of **5**. In both monomers of the asymmetric unit, this side chain is oriented toward the opening of the binding site. In monomer A, the O12 of **5** interacts with Gln120 and Asp123 through an ordered water molecule; no interactions are observed for O13. In monomer B, O12 hydrogen-bonds directly with Asp123 and Gln120, while O13 hydrogen bonds to the backbone nitrogen of Val121 and the Nδ2 of Asn152. These are minor variations, and in both monomers, the structure of the AmpC/**5** complex is consistent with the design of these inhibitors, with the side chain at C5 facing out toward bulk solvent as it begins to climb out of the active site. The equivalent potency of **5** with respect to **1**, despite the new interactions that it makes, explained the desolvation costs of this polar side chain and its interactions with amino acids on or near the enzyme surface.

The structure of the AmpC/**5** complex suggested that substituents at position 5 can be accommodated by the enzyme, motivating a further round of synthetic elaboration. Parallel synthesis was used to introduce several different side chains (compounds **8**−**13**, **15**−**21**; Scheme 1B), while more classical synthetic methods were used for derivatives **14** and **22**−**24** (Scheme 1C). To establish synthetic conditions and to probe effects on affinity, three 5-aminomethyl derivatives of **1** (compounds **8**, **9**, **10**; Scheme 1) were synthesized. The 5-aminomethylene derivatives of **1** had a higher affinity for AmpC than did the 5-oxymethyl derivatives (K_i range was between 0.010 and 0.037 μM and 0.083−600 μM, respectively), whereas the 5-sulfanylmethyl derivative, **14**, had an intermediate

affinity (K_i 0.080 μM; Table 1). Based on these results, a small library of further 5-aminomethylene derivatives was synthesized (Scheme 1B).

The motivation for derivitization was to explore the role of solubility on cell activity, and whereas the clogP, and indeed the measured logP values for these compounds varied considerably, their affinities for the enzyme were in the same range, often slightly higher (worse), as that of the lead, compound **1**. The compound with the highest affinity in this new series, compounds **10** had binding affinity of 10 nM about 2.5 fold better than **1** (Table 1); this may reflect the relative hydrophobicity of these side chain. Conversely, compounds **6**, **7**, **13**, **15**−**17**, **21**, and **24** suffered a 10−30-fold drop in affinity against the enzyme, presumably reflecting details of steric fit and overall electrostatic complementarity. Most affected were those with cationic side chains, such as compounds **6**, **16**, **17**, and **24** (K_i values of 260 nM, 1000 nM, 2000 nM, and 170 nM, respectively), which find themselves in a site that is known to prefer anions.[13] Consistent with this view, the affinities are substantially better for compounds **8**, **9**, **10**, **18**, and **23**, where the same methylamino side chains, in reason of their basicity, are neutral (K_i values range between 10 and 83 nM).

Modeling Inhibitor Lipophilicity and Membrane Permeability. A guiding hypothesis for this study was that the cell efficacy of the lead compound **1** is reduced by its low solubility and low bacterial membrane permeability. To model these effects in detail, we wanted to correlate the physical properties of **1** and its derivatives with their membrane permeability and their cellular activities. We began by computing pK_a, LogP, and LogD values for the compounds using the software ACDlab (Cambridgesoft, www.acdlabs.com), which was first experimentally validated for the benzo[*b*]thiophene-2-ylboronic derivatives.

In doing so, we found that the calculated pK_a values[22] for the boronic acid group was different than what we experimentally determined; this presumably reflects under-parametrization of this group in the program. The pK_a value of 6.4 used as reference for the boronic group of benzo[*b*]thiophene-2-ylboronic acid derivatives was determined experimentally. To evaluate how substitutions at position 5 in compound **1** effects boronic group ionization, pK_a for compound **7** has been measured (pK_a 6.6). Comparison between pK_a values of **1** and **7** showed that the presence of a substituent in position 5 in compound **1** does not change the pK_a value for the boronic group in position 2 of the molecule (Table 1).

Moreover, a comparison between pK_a measured for compound **1** with respect to the TH2B (pK_a 7.2) provided that the presence of phenyl ring decreases the acidity of the boronic group.

For selected compounds, experimental LogP values were determined through classical shake and flask and RP-LC analytical method. The experimental results were compared with the predicted values, and the two values were always close. Calculated LogP values for the library derivatives ranged from a minimum of 2.42 (±0.80; compound **6**) to a maximum of 6.71 (±0.82; compound **12**; Table 1)**.** Because the ACDlab software did not predict correctly the pK_a value for the boronic acid, it is reasonable to expect that also calculated LogD values are not correct. LogD values for compound **1** were directly obtained from the measured LogP and experimental pK_a values, applying the suitable equation and then comparing with the simulated one. cLogD at pH 7.4, experimentally derived for compound **1**, was found to be 4.8, and the ACD lab software value was 3.39.
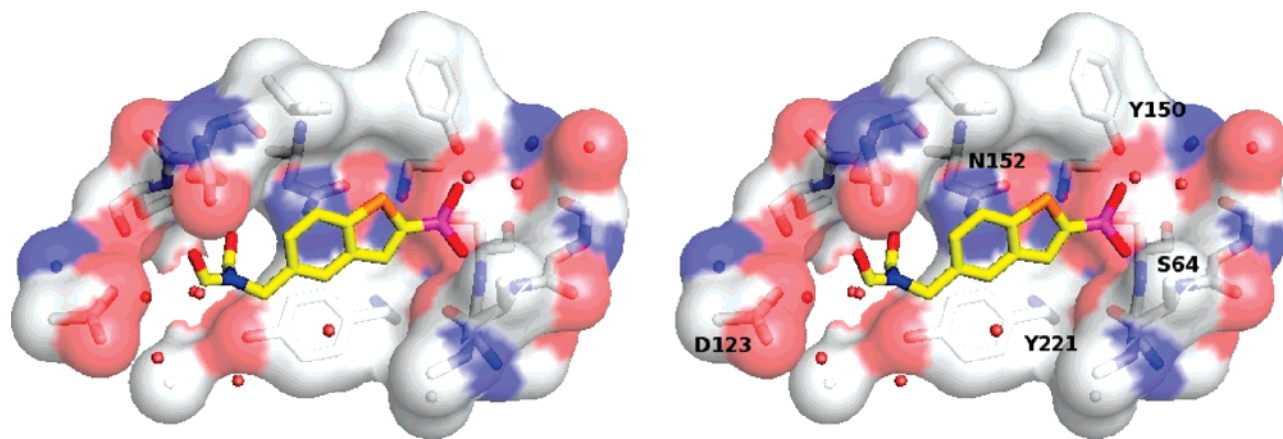
Figure 4. Stereoview of the AmpC/**5** complex. Red spheres represent water molecules; only monomer 2 of the asymmetric unit is shown for brevity. A transparent solvent accessible surface is shown for the enzyme, colored by atom type.

Table 4. Index of Permeability (iP) for Some 5-BZBTH2B Derivatives

cmpd	MIC amp (μg/mL)	MIC app. inhibitor (μM)	iP
1	32	359	7×10^{-5}
2	16	117	26×10^{-5}
3	16	91	33×10^{-5}
4	32	308	14×10^{-5}
5	16	92	40×10^{-5}
6	32	221	117×10^{-5}
8	16	78	47×10^{-5}
10	64	147	7×10^{-5}
14	32	84	95×10^{-5}
19	64	314	80×10^{-5}
22	16	92	30×10^{-5}
23	16	94	87×10^{-5}
24	16	117	145×10^{-5}

To derive exact cLogDs, which depend on ionization state, based on the experimentally measured pK_a values, we should simply adjust the cLogD value predicted by the program by a constant 1.4 units for the 5-MeBTH series. As relative values of LogDs for the series of derivatives, we reported cLogD at pH 7.4 that varied over 6 units (−0.31 for compound **23** to 6.30 for compound **12**; Table 1).

Structure−Membrane Affinity Relationship through Capacity Factor (Logk$^I_{IAM}$). We then looked to correlate membrane permeation with these physical properties, using an IAM.PC HPLC system to model partition coefficients. Artificial membranes provide an amphiphilic microenviroment similar to that in biological membranes, implicitly taking ionic effects into account and thus returning a more realistic model for passive membrane diffusion than the more widely used cLogP. Naturally, there are caveats on the interpretation of IAM.PC chromatography as a model for permeation: the method works best when equilibrium partitioning is rate-limiting in compound entry and exit from cell membranes, and surface adsorption may not result in drug permeation because the solute only binds to the polar head groups and never diffuses into the IAM hydrocarbon region. Thus, the molecular state responsible for absorption must be correlated with permeation to derive a structure−permeation relationship.
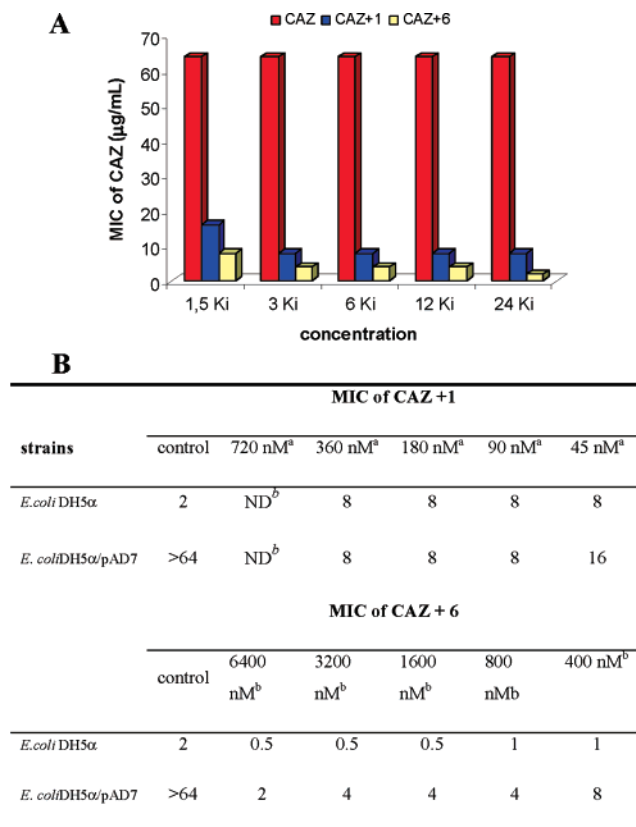
The membrane retention parameters, expressed as Logk$^I_{IAM}$, were determined for characteristic compounds, with all values measured at a pH of 3 (Table 4). This choice of pH was a matter of experimental convenience: at this value, the lead compound **1** is uncharged, its boronic acid has a pK_a of 6.4, and so an appreciable Logk$^I_{IAM}$ can be measured. On the other hand, the ionizaton of the artificial membrane is not significantly affected at relative pH 7.4 because the pK_a of the phosphate ester is 1.5.

Compounds with better affinity toward the stationary phase (IAM.PC) are characterized by high retention time (transcellular diffusion). The compounds with the highest affinity were compounds **1** and **2**, with Logk$^I_{IAM}$ values of 1.19 and 1.54, respectively; no differences in retention time were detected between free boronic acid and pinacol ester, as expected. Compounds bearing a positive charge, such as **6** and **24**, had much lower retention times, typically by 1.5−2 log orders. Conformational properties of the C5 side chain may also contribute: thus, the thioether and ether derivatives (compounds **13**, **14**) had a lower retention time than did the more rigid amino-bridged compounds (**9**, **10**, **19**, **21**). Unexpectedly, there is little correlation between Logk$^I_{IAM}$ and cLogP or cLogD for many derivatives; the parameters reflect different characteristics of hydrophobicity.

The observation that the binding of compound **1** to the artificial membranes can only be detected at pH 3 and is insignificant at pH 7.4, where it is ionized, suggests a reason for the low cellular efficacy of this β-lactamase inhibitor. It is thought that compound **1** crosses the outer envelope of Gram negative bacteria cell by passive diffusion.[12] Our results suggest that the compound does so only when it is neutral, and at pH 7.4 very little of the compound will be in such a state, substantially reducing its ability to cross the membrane. Conversely, the low retention time of inhibitors like compound **6** suggests that they may have better cell permeation properties, giving them an advantage as agents to reverse antibiotic resistance, despite their intrinsically lower on-enzyme potency. This motivated us to relate enzyme affinity to antiobiotic potency with characteristic inhibitors.

Structure−Permeability Relationships in *Escherichia coli*. We investigated the relationship between permeation, enzyme affinity, and cell-efficacy using *E. coli* strains that express AmpC β-lactamase. Thirteen compounds were tested for their ability to potentiate the activity of ampicillin, and a few were tested in combination with CAZ, measuring the MIC of the primary β-lactam in the presence of the inhibitor (Table 4). All compounds potentiated ampicillin activity when tested at an ampicillin/inhibitor ratio of 1:2 w:w. The MIC of ampicillin was reduced (improved) by 8−32-fold against these bacteria, with the MIC falling from 512 μg/mL in the absence of inhibitor to between 16 and 64 μg/mL in the presence of the inhibitors, depending on their identities.

Most of the derivatives had better antiresistance activity than did the lead compound **1**, despite their often reduced enzyme potency. This improved activity may be measured in three ways. The simplest is based on the concentration of the compound

A

B

	MIC of CAZ +1				
strains	control	720 nM[a]	360 nM[a]	180 nM[a]	90 nM[a]	45 nM[a]
E.coli DH5α	2	ND[b]	8	8	8	8
E. coliDH5α/pAD7	>64	ND[b]	8	8	8	16

	MIC of CAZ + 6				
strains	control	6400 nM[b]	3200 nM[b]	1600 nM[b]	800 nMb	400 nM[b]
E.coli DH5α	2	0.5	0.5	0.5	1	1
E. coliDH5α/pAD7	>64	2	4	4	4	8

[a] Ceftazidime (resistance breakpoint >32μg/ml). [b] N.D.: not determined.

Bacterial inoculum 5x10^5 CFU/ml.

Figure 5. (Panel a) Activity in cell culture of lead compound **1** and derivative **6** at concentrations of 1.5-, 3-, 6-, 12-, and 24-fold their K_i values vs *E. coli* expressing AmpC β-lactamase. (Panel b) The same activity values in tabular form. N.D. = not determined due to low solubility. [a]Concentration of compound **1**. [b]Concentration of compound **6**.

necessary to achieve an ampicillin MIC at a fixed 1:2 ratio of β-lactam to inhibitor. By this metric, all derivatives were more potent than compound **1** (Table 4). For instance, 78 μM of compound **8** reduced the MIC of the antibiotic to 16 μg/mL from 512 μg/mL, a 5-fold lower concentration than required by compound **1** to achieve an ampicillin MIC of 32 μg/mL. A second metric compares the MIC value achieved at the fixed ratio of ampicillin to inhibitor. The MIC of ampicillin at a 1:2 ratio to compound **1** is 32 μg/mL; about half of the derivatives tested reduced this MIC to 16 μg/mL. A third metric considers the improvement of antibiotic potency using even higher ratios of β-lactam to inhibitor. A dilution series of the third generation CAZ was performed in combination with compound **1** present at different ratios of its enzymatic K_i value. The MIC of CAZ at 45 nM compound **1**, 1.5× K_i, was 16 μg/mL, falling to 8 μg/mL at 90 nM compound **1**, but not further for higher concentrations of this inhibitor, to its solubility limit. Conversely, the MIC of CAZ at 400 nM of compound **6**, 1.5× its K_i, was 8 μg/mL, falling to 4 μg/mL as the concentration of **6** was increased and reaching a minimum of 2 μg/mL at the highest concentration of **6** assayed, 6.4 μM, at which the concentration of the inhibitor showed no sign of precipitation (Figure 5). These differing metrics of activity each have implications for our understanding of the cellular behavior of this series of inhibitors, how it relates to their physical properties, and how they may be further improved.

To understand the origins of the improved efficacy of the new inhibitors relative to the lead, a useful ratio to consider is

one that compares the inhibitor K_i to its MIC value when combined with ampicillin, which we refer to as the index of permeability (iP = K_i/MIC$_{inhib}$). All of the derivatives have better iP values than does compound **1**, with improvements ranging from 2- to 25-fold. The compounds with the best indexes of permeability were **6** and **24**, with values of 117×10^{-5} and 145×10^{-5}, respectively, compared to that of 7×10^{-5} for compound **1**. Both molecules are cationic at physiologic pH, which will almost certainly influence their permeability. Conversely, the iP value of the compound **22** is much lower (Table 4). Taken together with the IAM.PC biochromatographic separation, which indicated that these charged compounds interacted worse than uncharged ones, the high relative permeability values of compounds **6** and **24** may reflect passage through the outer membrane via porin channels, the route that β-lactams themselves are thought to travel. This route would separate them from compound **1**, which is thought to passively diffuse through the membrane. For this series of inhibitors, structural variations strongly influence the route of cell entry, which appears to have as much or more to do with efficacy as does enzyme affinity. These results, then, speak to the first two metrics of efficacy, concentration of compound necessary to reduce the MIC of a β-lactam antibiotic, and the best potency of the β-lactam observed in combination with a given inhibitor.

Perhaps the best way to understand the third metric of efficacy, the maximum potency of a β-lactam (minimum MIC) in combination with rising a amount of β-lactamase inhibitor, this may be understood as a function of the physical properties of the inhibitors, combined with their biological features. Despite its much greater potency on the enzyme, compound **1** is only sparingly soluble and confronts a membrane that it finds relatively impermeable. On the other hand, compounds like **6** are much more soluble, allowing them to be sampled at higher concentrations, and, as it happens, also more membrane penetrant. As antibiotic resistance agents, these compounds are more "drug-like" than the lead compound **1**, notwithstanding the latter's higher affinity for β-lactamase. It should be possible to further exploit this structure-guided strategy, aiming to improve pharmacokinetic properties of these inhibitors much more than the traditional affinity, to further optimize these compounds for antibiotic efficacy.

Supporting Information Available: Elemental analysis. This material is available free of charge via the Internet at http://pubs.acs.org.

References

(1) Amicosante, G.; Oratore, A.; Joris, B.; Galleni, M.; Frere, J. M.; Van Beeumen, J. Chromosome-encoded β-lactamases of Citrobacter diversus. Interaction with β-iodopenicillanate and labeling of the active site. *Biochem. J.* **1988**, *254* (3), 891−893.

(2) Bennett, P. M.; Chopra, I. Molecular basis of beta-lactamase induction in bacteria. *Antimicrob. Agents Chemother.* **1993**, *37* (2), 153−158.

(3) Jacobs, C.; Frere, J. M.; Normark, S. Cytosolic intermediates for cell wall biosynthesis and degradation control inducible beta-lactam resistance in gram-negative bacteria. *Cell* **1997**, *88*, 823−832.

(4) Hanson, N. D.; Sanders, C. C. Regulation of inducible AmpC beta-lactamase expression among *Enterobacteriaceae*. *Curr. Pharm. Des.* **1999**, *5*, 881−894.

(5) Essack, S. Y. The development of beta-lactam antibiotics in response to the evolution of beta-lactamases. *Pharm. Res.* **2001**, *18* (10), 1391–1399.

(6) Philippon, A.; Arlet, G.; Jacoby, G. Plasmid-determined AmpC-type beta-lactamases. *Antimicrob. Agents Chemother.* **2002**, *46* (1), 1–11.

(7) Lobkovsky, E.; Billings, E. M.; Moews, P. C.; Rahil, J.; Pratt, R. F.; et al. Crystallographic structure of a phosphonate derivative of the *Enterobacter cloacae* P99 cephalosporinase: Mechanistic interpretation of a beta-lactamase transition-state analogue. *Biochemistry* **1994**, *33*, 6762–6772.

(8) Kumar, S.; Pearson, A. L.; Pratt, R. F. Design, synthesis, and evaluation of alpha-ketoheterocycles as class C beta-lactamase inhibitors. *Bioorg. Med. Chem.* **2001**, *9*, 2035–2044.

(9) Crichlow, G. V.; Nukaga, M.; Doppalapudi, V. R.; Buynak, J. D.; Knox, J. R. Inhibition of class C beta-lactamases: Structure of a reaction intermediate with a cephem sulfone. *Biochemistry* **2001**, *40*, 6233–6239.

(10) Tondi, D.; Powers, R. A.; Caselli, E.; Negri, M. C.; Blazquez, J.; et al. Structure-based design and in-parallel synthesis of inhibitors of AmpC beta-lactamase. *Chem. Biol.* **2001**, *8*, 593–611.

(11) Weston, G. S.; Blazquez, J.; Baquero, F.; Shoichet, B. K. Structure-based enhancement of boronic acid-based inhibitors of AmpC beta-lactamase. *J. Med. Chem.* **1998**, *41*, 4577–4586.

(12) Powers, R. A.; Blazquez, J.; Weston, G. S.; Morosini, M. I.; Baquero, F.; et al. The complexed structure and antimicrobial activity of a nonbeta-lactam inhibitor of AmpC beta-lactamase. *Protein Sci.* **1999**, *8*, 2330–2337.

(13) Powers, R. A.; Shoichet, B. K. Structure-based approach for binding site identification on AmpC β-lactamase. *J. Med. Chem.* **2002**, *45* (15), 3222–3234.

(14) Kettner, C. A.; Shenvi, A. B. Inhibition of the serine proteases leukocyte elastase, pancreatic elatase, cathepsin G, and chymotrypsin by peptide boronic acids. *J. Biol. Chem.* **1984**, *259*, 15106–15114.

(15) Otwinowski, Z.; Minor, W. Processing of X-ray diffraction data collected in oscillation mode. *Methods Enzymol.* **1997**, *276*, 307–326.

(16) Leslie, A. G. W.; Brick, P.; Wonacott, A. *Daresbury Laboratory Information Quarterly for Protein Crystallography*; Daresbury Laboratory: Warrington, U.K., 1986; 18, pp 33–39.

(17) Brunger, A. T.; Adams, P. D.; Clore, G. M.; DeLano, W. L.; Gros, P.; Grosse-Kunstleve, R. W.; Jiang, J. S.; Kuszewski, J.; Nilges, M.; Pannu, N. S.; Read, R. J.; Rice, L. M.; Simonson, T.; Warren, G. L. Crystallography and NMR system: A new software suite for macromolecular structure determination. *Acta Crystallogr., Sect. D: Biol. Crystallogr.* **1998**, *54*, 905–921.

(18) McRee, D. E. XtalView/XfitsA versatile program for manipulating atomic coordinates and electron density. *J. Struct. Biol.* **1999**, *125* (2–3), 156–165.

(19) Usher, K. C.; Blaszczak, L. C.; Weston, G. S.; Shoichet, B. K.; Remington, S. J. Three-dimensional structure of AmpC beta-lactamase from *Escherichia coli* bound to a transition-state analogue: Possible implications for the oxyanion hypothesis and for inhibitor design. *Biochemistry* **1998**, *37*, 16082–16092.

(20) Wayne, P. A. *Methods for dilution antimicrobial tests for bacteria that grow aerobically approved standard*, 4th ed.; NCCLS, National Committee for Clinical Laboratory Standards: Wayne, PA, 2000; NCCLS document M7–A5.

(21) Wayne, P. A. *Performance standards for antimicrobial susceptibility testing*; Clinical and Laboratory Standards Institute: Wayne, PA, 2005; CLSI document M100–S15.

(22) Gans, P.; Sabatini, A.; Vacca, A. *Ann. Chim.* **1999**, *89*, (Società chimica italiana).

(23) Silva, C.; Mor, M.; Vacondio, F.; Zuliani, V.; Plazzi, P. pH-partition profiles of 4-(3-oxo-1,2-benzisothiazolin-2-yl)phenyl and phenoxy-alkanoic acids. *Farmaco* **2003**, *58*, 989–993.

(24) Smith, D. A.; Van de Waterbeemd, H. Pharmacokinetics and metabolism in early drug discovery. *Curr. Opin. Chem. Biol.* **1999**, *3*, 373–378.

(25) Lipinski, C. A.; Lombardo, F.; Dominy B. W.; Paul J. Feeney P. J. Experimental and computational approaches to estimate solubility and permeability in drug discovery and development setting. *Adv. Drug Delivery Rev.* **2001**, *46*, 3–26.